DOI:
10.1037/neu0000393

Document Version
Peer reviewed version

Neural correlates of audiovisual sensory integration

Jia Huang[1,2†], Antje A. T. S. Reinders[3†], Ya Wang[1], Ting Xu[1], Ya-wei Zeng[4], Ke Li[4], Rowena Handley[5], Eric F. C. Cheung[6], Raymond C. K. Chan[1, 2*], Paola Dazzan[3*]

1: Neuropsychology and Applied Cognitive Neuroscience Laboratory, CAS Key Laboratory of Mental Health, Institute of Psychology, Beijing, China

2： Department of Psychology, University of Chinese Academy of Sciences, Beijing, China

3: Department of Psychosis Studies, Institute of Psychiatry, Psychology and Neuroscience, King's College London, London, UK

4: MRI Imaging Center, 306 Hospital, Beijing, China

5: Bristol-Myers Squibb, UK

6: Castle Peak Hospital, Hong Kong, China

† Both authors contributed equally to this manuscript.

*: corresponding author

Raymond C. K. Chan

Tel/Fax: 86(10)64836274

Email: rckchan@psych.ac.cn

Postal address: Room 526, South Building, Institute of Psychology, Chinese Academy

of Sciences, 16 Lincui Road, Beijing 100101, China

Or

Paola Dazzan,

Tel.: Tel +44 (0)207 848 0590; Fax +44 (0)207 848 0287

Email: paola.dazzan@kcl.ac.uk

Postal address: Department of Psychosis Studies, PO 40, Institute of Psychiatry, De Crespigny Park, London SE5 8AF

Acknowledgements:

This work was supported by grants from the Beijing Municipal Science & Technology Commission Grant (Z161100000216138), the Beijing Training Project for Leading Talents in Science & Technology (Z151100000315020), the National Science Fund China Distinguished Young Investigator Award (81088001), the "Strategic Priority Research Program (B)" of the Chinese Academy of Sciences (XDB02030002) and the CAS/SAFEA International Partnership Programme for Creative Research Teams (Y2CX131003) to Raymond Chan; and grants from the Young Investigator Scientific Fund of the Institute of Psychology, the Mental Health Key Laboratory of the Chinese Academy of Sciences and the National Science Fund China (31100747) to Jia Huang. These funding agents had no further role in the study design; in the collection, analysis and interpretation of the data; in the writing of the manuscript; and in the decision to submit the paper for publication. B. Armstrong is acknowledged for technical assistance during task programming.

Abstract:

Objective: The present study aimed to investigate the neural basis of information matching during sensory integration using a spatial-temporal matching task in healthy individuals.

Method: A total of 37 healthy participants were recruited to match spatial dots with an auditory tone sequence in a 3T GE Discovery MR750 scanner. In addition, they were examined with the sensory integration subscale of the Cambridge Neurological Inventory (CNI).

Results: We found that the bilateral occipital-parietal conjunction cortex and the precentral frontal gyrus were activated during the matching condition rather than in the non-matching condition. Activation of the occipital-parietal conjunction cortex was associated with integration of information across visual and auditory modalities, while activation of the precentral frontal gyrus was associated with decision-making of movements. In addition, activation of the left superior frontal gyrus was associated with scores on the sensory integration subscale of the CNI.

Conclusions: These findings suggest that the bilateral occipital-parietal conjunction cortex is responsible for matching information input from multiple modalities during audiovisual sensory integration.

Keywords: sensory integration, audiovisual, occipital-parietal conjunction cortex, functional neuroimaging

Public Significance Statements

This study aimed to examine information matching during audiovisual sensory integration with a spatial-temporal matching task using functional imaging in healthy volunteers. The findings suggest that the bilateral occipital-parietal conjunction cortex is responsible for matching information input from multiple modalities during audiovisual sensory integration. These findings have clinical implications for the understanding of the underlying neural mechanism of sensory integration in schizophrenia and autism spectrum disorders.

Introduction

Neurological soft signs (NSS) represent a group of non-localizable neurological abnormalities, including dysfunction in the execution of simple motor coordination, complex motor sequencing and sensory integration tasks (Alain et al. 1998; Zhang et al. 2015; Wang et al. 2016). Although their pathophysiological basis remains unclear, they have been consistently reported in excess in individuals with psychiatric disorders of possible neurodevelopmental origin like schizophrenia. Among these signs, deficits in the ability to integrate signals from different sensory modalities are particularly important, as this ability plays a crucial role in the cognitive representation of the outside world. Investigating the neural basis of sensory integration in clinical and non-clinical populations is therefore important not only to advance our understanding of its neuropathological substrate, but also our understanding of its role in the pathophysiology of psychiatric disorders.

The precise relationship between NSS and brain alterations is not clear (Chen et al. 1995). Over the last decade, increasing evidence has shown that NSS are associated with diffuse cortical and subcortical alterations in brain structure and functional networks (Dazzan et al. 2004; Zhao et al. 2014). For example, more sensory integration signs were associated with grey matter volume reduction of the inferior frontal gyrus, the right middle and superior temporal gyrus, and the bilateral anterior cingulate gyri in healthy individuals (Dazzan et al. 2006). Sensory integration deficits in first-episode psychosis was additionally associated with grey matter volume reduction in the right precentral gyrus, the adjacent inferior frontal gyrus, the

left superior temporal gyrus, the insula and subcortical regions such as the bilateral lenticular nucleus, the thalamus and the pulvinar (Dazzan et al. 2004; Heuser et al. 2011). Functionally, previous studies have mainly focused on the subgroups of NSS such as motor coordination such as the Fist-Edge-Palm task (Chan et al. 2006; Chan et al. 2015), the finger tapping task {Muller, 2002 #6992} and the pronation/supination task {Schroder, 1999 #6993}. On the other hand, many fMRI studies have examined disinhibition using the go/no-go paradigm (see Zhao et al. 2014 for review). However, relatively few studies have examined the functional neural substrates of sensory integration as a subgroup of NSS. Narrowing down to one specific construct will be helpful in disentangling whether there are specific or diffuse functional brain alterations underlying sensory integration deficits. Deficits in sensory integration mainly manifest as impaired audio-visual integration, bilateral extinction, agraphaesthesia and astereognosis (Dazzan 2002). Audio-visual integration sign tested in the Neurological Evaluation Scale (NES) provides a suitable construct to measure the ability to integrate spatial and temporal information simultaneously signaled by different sensory modalities. The aim of the present study was to identify the functional brain correlates of audio-visual integration.

Since the audio-visual integration sign tested in the NES requires the processing of spatial spacing and temporal interval information integration, it is possible that activation of the lateral intraparietal cortex is involved (Andersen 1997; Sestieri et al. 2006; Nardo et al. 2013). Guterstam et al. (2013) found that visual-tactile stimulation congruent in time and space activates the bilateral ventral premotor and bilateral

intraparietal cortices, which suggests that the integration of temporally and spatially congruent multisensory signals in a premotor-intraparietal circuit could be sufficient for visual-tactile integration. The combination of auditory and visual stimuli may however be processed by different cortical networks (Vander Wyk et al. 2010). For example, compared with desynchronized audio-visual stimuli pairing, synchronized audio-visual stimuli seem to lead to a larger signal change in the claustrum region, in addition to an activation of the superior temporal gyrus and the inferior frontal gyrus (Olson et al. 2002; Biau et al. 2016). Additionally, in the presence of emotionally incongruent audio-visual stimuli, the right temporo-parietal junction and the right superior frontal gyrus have been found to be more activated than in the presence of emotionally congruent stimuli (Muller et al. 2011).

In addition to the parietal cortex, the temporal and frontal cortices could also play important roles in audiovisual integration (Plank et al. 2012; Paraskevopoulos et al. 2014). For example, Plank et al (2012) found significant activation at the right middle and superior temporal gyri when the localization of the auditory sound sources were spatially congruent with semantically matched visual stimuli. Studies that have evaluated activation when non-verbal stimuli are presented have found that the bilateral inferior frontal gyri were responsible for integrating unfamiliar artificial sounds and images, while the bilateral superior temporal gyri were involved in integrating familiar artificial sounds and images (Naumer, 2009). Moreover, these authors found evidence of frontal involvement, with an increased activation in the left inferior frontal gyrus in association with sound-source localization performance.

However, it remains unclear how sensory signals are integrated when spatial information from the visual modality and temporal information from the auditory modality are presented simultaneously.

To better understand the neural basis of audiovisual sensory integration, we investigated information matching during audiovisual sensory integration with a spatial-temporal matching task using functional Magnetic Resonance Imaging. Based on the audio-visual integration test in the NES (Buchanan and Heinrichs 1989), we developed a novel dot-tone matching paradigm, in which participants had to choose the dot matrix that best matches the tone sequence when the dot matrix and tone sequence were presented simultaneously. We additionally examined which brain regions were correlated with behavioural performance on sensory integration signs assessed with the Cambridge Neurological Inventory (CNI) (Chen et al. 1995). Based on previous evidence, we hypothesized that the differential neural response between matching conditions and non-matching conditions would involve advanced sensory association cortices, such as the lateral intraparietal cortex and bilateral frontal regions.

Method

Participants:

A total of 37 participants (20 males, mean $\pm$ SD: age 19.08 $\pm$ 1.57; education: 12.81 $\pm$ 1.43 years) were recruited from the local community in Beijing, China, through internet advertisement. All participants had normal (or corrected to normal)

vision and normal hearing. The inclusion criteria were: a) age >= 18; and b) full understanding of the task requirement. Exclusion criteria included a personal or family history of psychiatric disorder, a history of neurological disorder, and a history of substance abuse. All participants were right-handed and their head motions were within 1.5mm and 1.5 degree. All participants gave informed consent prior to their participation in accordance with the protocol approved by the Ethics Committee of the corresponding institutions.

Procedure:

We developed a dot matrix and tone sequence matching task to capture spatial-temporal matching (Figure 1). Visual stimuli presented in each trial consisted of an instruction sentence lasting for one second. An auditory tone sequence was presented simultaneously with three choices of dot matrix. The duration of each tone sequence was 3.65 seconds. The duration of each tone or each silent tone was 350ms. The tone interval was 200ms. The number of tones in each sequence ranged randomly from three to six. After the tone sequence, the visual dot matrix choices would remain for 550ms. In the matching condition, participants were required to choose in the dot matrix the spatial character that was congruent with the temporal character of the tone sequence. For example, the dot matrix "•• … •…•" should be matched with the tone sequence like "Du Du … Du …Du". In the control condition, participants were required to choose the dot matrix with a square in front, which was incongruent with the tone sequence. In the control condition, no matching process

was required.

Each matching or control block contained five trials. An instruction requesting the participant to make a response such as ‘choose the matching matrix’ or ‘choose the matrix with a square’ was presented prior to starting the paradigm and during each block of the trial. Between each block, a fixation at the centre of the screen lasting for 18 seconds acted as the resting block to wash out the effect of the last condition. The experiment consisted of five blocks of matching condition, five blocks of control condition and 10 blocks of resting condition. The total task time was 7.3 min. An angled mirror above the participants’ eyes showed the stimuli, which were projected onto a screen in the bore of the magnet behind the participants’ head. Stimuli presentation was controlled with the Eprime computer programme (Psychology Software Tools, Inc.).

INSERT FIGURE 1 HERE

After scanning, all participants were evaluated by a researcher with the NSS subscales of the Cambridge Neurological Inventory (CNI) (Chen et al. 1995). These include the sensory integration subscale capturing conventional clinical assessment of sensory integration signs such as left-right discrimination, extinction and astereognosis, as well as the motor coordination (e.g., fist-edge-palm, rapid finger tapping) and disinhibition signs (e.g., go/no-go, saccade head movement).

Imaging data acquisition:

Functional and structural MRI were acquired with a Siemens 3T (SIEMENS 3T-Trio A Tim, Erlangen, Germany) MRI whole body scanner using a 32-channel head coil. Functional images were obtained using a T2-weighted single-shot gradient echoplanar imaging (EPI) sequence (TR: 2000, TE: 30, 90^{o} flip angle, FOV: 210mm, matrix: 64X64, voxel size: 3.3X3.3X4mm^3). Each EPI volume contained 32 axial slices (thickness 4mm, 0mm gap), acquired in interleaved order, covering the whole brain. Each run contained 243 functional images. The first three slices of each run were discarded to allow for T1 equilibration. In addition, a high-resolution T1-weighted magnetization-prepared rapid gradient-echo imaging (MP-RAGE) 3D MRI sequence was obtained from each participant (TR: 2300ms, TE: 3.01ms, 9 flip angle, FOV: 240X256, matrix: 256X256, voxel size: 1X1X1 mm^3).

Imaging data analysis:

Imaging data were analyzed with the SPM8 software package (SPM8; Wellcome Department of Imaging Neuroscience, London, UK) implemented in Matlab 2009b (Mathworks Inc., Sherborn, MA, USA). Three dummy scans at the beginning of the measurement were removed automatically from the dataset. Pre-processing included motion correction (realignment) with the function of 'estimate and reslice'. Images were registered to the first ICBM 152, which was an anatomical template created by the Montreal neurological Institute (MNI) based on 152 brains with a 2X2X2 mm resolution. The images were then spatially smoothed by an isotropic Gausian Kernel

with FWHM of 8mm.

For statistical analysis using the General Linear Model, individual design matrices were generated. A matrix consisted of one session with one regressor for the matching condition and the other regressor for the control condition. A boxcar model function of every condition was convolved with the canonical haemodynamic response function (HRF). The signal time course was high-pass filtered (128s). Parameter estimates were subsequently calculated for each voxel using weighted least squares to provide maximum likelihood estimates based on the non-sphericity assumption of the data in order to obtain identical and independently distributed error terms. T-test was carried out for every voxel to compare the BOLD activity between matching and control conditions. At the individual participant level, two different contrasts were calculated: matching condition > control condition and control condition > matching condition.

The first calculated contrast was entered into the second-level random effects analysis. The two contrasts were thresholded at $p<0.001$ (FWE corrected) to correct for multiple comparisons at the cluster level. In addition, a regression analysis was conducted, correlating the performance of each participant in the sensory integration subscale of the CNI to the BOLD response for the contrast 'matching>control' by adding the sensory integration subscale score of the CNI into the second-level model. We used a threshold of $p<0.001$ at the voxel level and a p value of $p<0.05$ alphasim corrected at the cluster level using the updated alphasim version in DPABI (Yan et al. 2016). Region of interest (ROI) analysis were performed

using the Marsbar (Brett et al. 2002) to obtain parameter estimates for the condition 'matching > control' in significant clusters.

Results

The mean accuracy of the behavioural performance in the matching condition was 0.81 ± SD = 0.03. The subscale scores measured for motor coordination, sensory integration and disinhibition of the CNI were 1.03 ± 1.19, 0.84 ± 0.93, and 0.97 ± 1.11, respectively. The results of the random-effects analysis of the fMRI findings are presented in Figure 2 for the contrasts between matching and control conditions. The corresponding locations of these activated clusters are described in detail in Table 1.

Regions in the occipital-parietal junction and the frontal lobe exhibited more activation in the matching condition than in the control condition. In addition, the left posterior cingulate gyrus, the temporal gyrus and the left superior frontal gyrus were observed to be inhibited in the matching condition.

The largest cluster in Table 1 mainly included the parietal lobe (5620 voxels), the precuneus (2006 voxels), the temporal lobe (972 voxels), the middle occipital lobe (1066 voxels), the right cerebellum (1359 voxels) and the left cerebellum (1681 voxels). To confirm that the activation in this largest cluster was mainly due to activation in the parietal, occipital and its conjunction lobe, we defined the parietal and occipital parts of this largest cluster according to the AAL anatomical template. Three regions of interest (ROIs) were defined. The first region was defined according to the largest activation cluster as indicated in Table 1. The second region was

defined by the intersection of this largest activation cluster and an AAL anatomically defined cluster of the right superior parietal lobe (yellow in Figure 3). The third region was defined by the intersection of the largest activation cluster and AAL anatomically defined cluster of the right middle occipital lobe (purple in Figure 3). The activation area of this largest cluster involved both the parietal and occipital lobes. This was therefore labeled as the right occipital-parietal conjunction.

In a separate post-hoc analysis, we explored whether scores on the sensory integration subscale of the CNI were correlated with brain activation in the regions reported above. We used the CNI sensory integration subscale score as a regressor variable in the second-level analysis. A regression analysis of the second-level contrast 'MATCHING-CONTROL'('MAT-CON') yielded a significant inverse correlation (Spearman's $r=-0.559$, $p<0.001$) between the mean amplitude of the BOLD response in the left superior frontal lobe and the sensory integration subscale score of the CNI. The significant cluster of activation was located mainly in the left superior frontal gyrus (MNI coordinates of peak voxel (x,y,z)=-40 56 -2; T value=4.45, cluster size=114, $p<0.05$, alphasim corrected, Figure 4). Here, poorer sensory integration ability was associated with elevated activation in this cluster in the matching-control contrast (see Figure 3, scatter plot).

INSERT FIGURE 2 HERE

INSERT TABLE 1 HERE

INSERT FIGURE 3 HERE

INSERT FIGURE 4 HERE

Discussion

In this study, we investigated neural activation during visual and auditory sensory integration by matching an auditory tone with a dot matrix presented spatially. Our findings suggest that the bilateral occipital-parietal conjunction cortices and frontal regions may be responsible for matching information input from multiple sensory modalities and may thus be sensitive to audiovisual sensory integration. The left frontal lobe may additionally be involved in general sensory-integration performance. These brain regions may represent neural correlates of visual-audio sensory input integration based on temporal spatial congruency. Our results also suggest that the performance of sensory integration tasks commonly included in the examination of NSS in clinical and non-clinical populations involve the frontal cortex.

We found that when matching spatial information from a visual input with temporal information from an auditory input, the occipital-parietal conjunction was activated. This is consistent with previous findings suggesting that activation of the intraparietal cortex is associated with spatial congruency in sensory integration (Sestieri et al. 2006; Plank et al. 2012). In another study, congruent audiovisual stimuli elicited activity in the fronto-temporal and occipital areas, while incongruent stimuli activated temporal and parietal regions (Paraskevopoulos et al. 2014). Our finding also highlights the role of a distributed posterior cortical network, particularly in the right hemisphere, that integrates spatial spacing information and temporal interval information. In the paradigm we used, the auditory inputs were tone sequences, in which information was conveyed temporally, while the visual inputs

were represented by dot matrices, in which information was conveyed spatially. In contrast to a previous study in which information were matched semantically (Plank et al. 2012), here we focused on the congruence between spatial spacing and temporal interval. Such congruence was correlated with activation in the occipital-parietal conjunction, especially in the right superior parietal cortex. Activation in the occipital cortex is related to the strength of the visual input. The superior parietal cortex is involved in spatial attention shift and visual feature conjunction (Corbetta et al. 1995; Okada and Hickok 2009), both during the manipulation of information in working memory (Koenigs et al. 2009) and during sensory-motor integration (Wolpert et al. 1998; Iacoboni 2004). It is possible that in our experiment the superior parietal cortex became activated because participants had to shift attention to choose between multiple dot matrices, combine this visual feature with the auditory tone sequence, keep updating spatial and temporal information using working memory, maintain internal representation and finally trigger motor key-pressing. In this sense, our findings provide evidence for the neural mechanisms that underlies the integration of spatial temporal information.

When we examined the correlates of general sensory integration ability with the CNI, we found that worse performance on this test was correlated with decreased activation of the left superior frontal lobe. However, it should be noted that in the CNI examination, sensory integration is assessed by multiple tactile stimuli rather than with audiovisual inputs as in our fMRI paradigm. For audiovisual sensory integration, two potential cortical mechanisms have been proposed: a “direct”

sensory-sensory interaction, and an “indirect” sensory-motor interaction (Okada and Hickok 2009). In the “direct” sensory-sensory interaction, the visual information would be integrated with the auditory information in the superior temporal and parietal gyri via projections from the sensory input systems in the occipital lobe and the temporal lobe. In the “indirect” sensory-motor interaction, the visual-auditory information would be integrated and represented in the frontal lobe via the parietal lobe. Our finding of left frontal lobe activation in the contrast of matching condition versus non-matching condition supports the second mechanism. The left frontal lobe could have been involved in mapping the representation of information after auditory-visual integration onto the key pressing motor choice. Previous studies have suggested that even NSS may have specific structural or functional localizations (Dazzan et al. 2004; Zhao et al. 2014), but few studies have specifically investigated the neural basis of visual-auditory integration. Our study provides preliminary evidence of where visual-auditory information is integrated in the brain and how specific activation in the frontal region may be related to general sensory integration ability.

It is however important to highlight some limitations to our study. First, the paradigm used was a block-design that provides results with high signal-noise ratio compared to an event-related design. However, such a design makes it impossible to disentangle at which stage of the processing the integration part occurs in the temporal framework. Further work should examine effective connectivity between cortical regions to compensate for the lack of temporal information. Second, it is

possible that the control and matching conditions had different levels of difficulty in capturing the proposed sensory integration. The matching task would require paying active attention to the auditory stimuli and thus could have exerted demand on working memory. Therefore, in future studies the control condition should be modified to establish better baseline activity. Taken together, our findings suggest that the bilateral occipital-parietal conjunction cortex may be responsible for matching information input from multiple modalities and may therefore be sensitive to audiovisual sensory integration. Moreover, we propose that the left frontal lobe is involved in another neural mechanism for sensory integration, associated with mapping information representation after integration onto motor decision. Future studies could refine the paradigm proposed, and make it useful for the evaluation of spatial-temporal information matching in clinical populations, to investigate the underlying neural mechanism of sensory integration.

References

Alain C, Woods DL, Knight RT. 1998. A distributed cortical network for auditory sensory memory in humans. Brain Res. 812:23-37.

Andersen RA. 1997. Multimodal integration for the representation of space in the posterior parietal cortex. Philosophical Transactions of the Royal Society B: Biological Sciences 352:1421-1428.

Biau E, Moris Fernandez L, Holle H, Avila C, Soto-Faraco S. 2016. Hand gestures as visual prosody: BOLD responses to audio-visual alignment are modulated by the communicative nature of the stimuli. NeuroImage 132:129-137.

Brett M, Anton J-L, Valabregue R, Poline JB. 2002. Region of interest analysis using an SPM toolbox[abstract]. Presented at the 8th International Conference on Functional Mapping of the Human Brain, June 2-6, Sendai, Japan. Available on CD-ROM in NeuroImage 16:No 2.

Buchanan RW, Heinrichs DW. 1989. The neurological evaluation scale (NES): A structured instrument for the assessment of neurological signs in schizophrenia. Psychiatry Res. 27:335-350.

Chan RC, Huang J, Zhao Q, Wang Y, Lai YY, Hong N, Shum DH, Cheung EF, Yu X, Dazzan P. 2015. Prefrontal cortex connectivity dysfunction in performing the Fist-Edge-Palm task in patients with first-episode schizophrenia and non-psychotic first-degree relatives. NeuroImage. Clinical 9:411-417.

Chan RC, Rao H, Chen EE, Ye B, Zhang C. 2006. The neural basis of motor sequencing: an fMRI study of healthy subjects. Neurosci. Lett. 398:189-194.

Chen EY, Shapleske J, Luque R, McKenna PJ, Hodges JR, Calloway SP, Hymas NF, Dening TR, Berrios GE. 1995. The Cambridge Neurological Inventory: a clinical instrument for assessment of soft neurological signs in psychiatric patients. Psychiatry Res. 56:183-204.

Chen EYH, Shapleske J, Luque R, McKenna PJ, Hodges JR, Calloway SP, Hymas NFS, Dening TR, Berrios GE. 1995. The Cambridge Neurological Inventory: A clinical instrument for assessment of soft neurological signs in psychiatric patients. Psychiatry Res. 56:183-204.

Corbetta M, Shulman GL, Miezin FM, Petersen SE. 1995. Superior Parietal Cortex Activation During Spatial Attention Shifts and Visual Feature Conjunction. Science 270:802-805.

Dazzan P. 2002. Neurological soft signs in first-episode psychosis: a systematic review. The British Journal of Psychiatry 181:50s-57.

Dazzan P, Morgan KD, Chitnis X, Suckling J, Morgan C, Fearon P, McGuire PK, Jones PB, Leff J, Murray RM. 2006. The structural brain correlates of neurological soft signs in healthy individuals. Cereb. Cortex 16:1225-1231.

Dazzan P, Morgan KD, Orr KG, Hutchinson G, Chitnis X, Suckling J, Fearon P, Salvo J, McGuire PK, Mallett RM, Jones PB, Leff J, Murray RM. 2004. The structural brain correlates of neurological soft signs in AESOP first-episode psychoses study. Brain 127:143-153.

Guterstam A, Gentile G, Ehrsson HH. 2013. The Invisible Hand Illusion: Multisensory Integration Leads to the Embodiment of a Discrete Volume of Empty Space. J. Cognit. Neurosci.:1-22.

Heuser M, Thomann PA, Essig M, Bachmann S, Schröder J. 2011. Neurological signs and morphological cerebral changes in schizophrenia: An analysis of NSS subscales in patients with first episode psychosis. Psychiatry Research: Neuroimaging 192:69-76.

Iacoboni M. 2004. Interhemispheric visuo-motor integration in humans: the role of the superior parietal cortex. Neuropsychologia 42:419-425.

Koenigs M, Barbey AK, Postle BR, Grafman J. 2009. Superior Parietal Cortex Is Critical for the

Manipulation of Information in Working Memory. J. Neurosci. 29:14980-14986.
Muller VI, Habel U, Derntl B, Schneider F, Zilles K, Turetsky BI, Eickhoff SB. 2011. Incongruence effects in crossmodal emotional integration. NeuroImage 54:2257-2266.
Nardo D, Santangelo V, Macaluso E. 2013. Spatial orienting in complex audiovisual environments. Hum. Brain Mapp. 35:1597-1614.
Okada K, Hickok G. 2009. Two cortical mechanisms support the integration of visual and auditory speech: A hypothesis and preliminary data. Neurosci. Lett. 452:219-223.
Olson IR, Gatenby JC, Gore JC. 2002. A comparison of bound and unbound audio-visual information processing in the human cerebral cortex. Brain Res. Cogn. Brain Res. 14:129-138.
Paraskevopoulos E, Kuchenbuch A, Herholz SC, Foroglou N, Bamidis P, Pantev C. 2014. Tones and numbers: a combined EEG-MEG study on the effects of musical expertise in magnitude comparisons of audiovisual stimuli. Hum. Brain Mapp. 35:5389-5400.
Plank T, Rosengarth K, Song W, Ellermeier W, Greenlee MW. 2012. Neural correlates of audio-visual object recognition: effects of implicit spatial congruency. Hum. Brain Mapp. 33:797-811.
Sestieri C, Di Matteo R, Ferretti A, Del Gratta C, Caulo M, Tartaro A, Olivetti Belardinelli M, Romani GL. 2006. “What” versus “Where” in the audiovisual domain: An fMRI study. NeuroImage 33:672-680.
Vander Wyk BC, Ramsay GJ, Hudac CM, Jones W, Lin D, Klin A, Lee SM, Pelphrey KA. 2010. Cortical integration of audio-visual speech and non-speech stimuli. Brain Cogn. 74:97-106.
Wang X, Cai L, Li L, Yang Y, Yao S, Zhu X. 2016. Neurological soft signs in Chinese adolescents with antisocial personality traits. Psychiatry Res. 243:143-146.
Wolpert DM, Goodbody SJ, Husain M. 1998. Maintaing internal representations: the role of the human superior parietal lobe. Nat. Neurosci. 1:529-533.
Yan CG, Wang XD, Zuo XN, Zang YF. 2016. DPABI: Data Processing & Analysis for (Resting-State) Brain Imaging. Neuroinformatics 14:339-351.
Zhang J, Cai L, Zhu X, Yi J, Yao S, Hu M, Bai M, Li L, Wang Y. 2015. Neurological soft signs in adolescents with borderline personality traits. International journal of psychiatry in clinical practice 19:40-44.
Zhao Q, Li Z, Huang J, Yan C, Dazzan P, Pantelis C, Cheung EFC, Lui SSY, Chan RCK. 2014. Neurological soft signs are not "soft" in brain structure and functional networks: Evidence from ALE meta-analysis. Schizophr. Bull. 40:626-641.

Table 1: fMRI activation in the matching-control and control-matching contrasts (FWE corrected p <0.001, k=20, L = Left, R = Right)

Brain region	k	T	x y z(MNI)
Matching > Control(MAT-CON)			
Occipital-parietal cortex	14978	16.67	32 -70 38
R middle frontal gyrus	1824	14.71	48 10 30
L frontal lobe	2390	12.6	-46 2 34
R inferior frontal gyrus	487	11.88	32 28 0
Medial frontal gyrus	931	11.28	-4 10 54
Left caudate	590	8.94	-18 -6 18
R superior frontal gyrus	139	8.71	46 42 24
R thalamus	438	8.13	16 -6 18
Control>Matching(CON-MAT)			
L posterior cingulate	256	9.18	-8 -60 28
L middle temporal gyrus	190	8.34	-52 -68 28
R superior temporal gyrus	44	8.3	60 -64 24
L superior frontal gyrus	118	7.62	-16 50 40

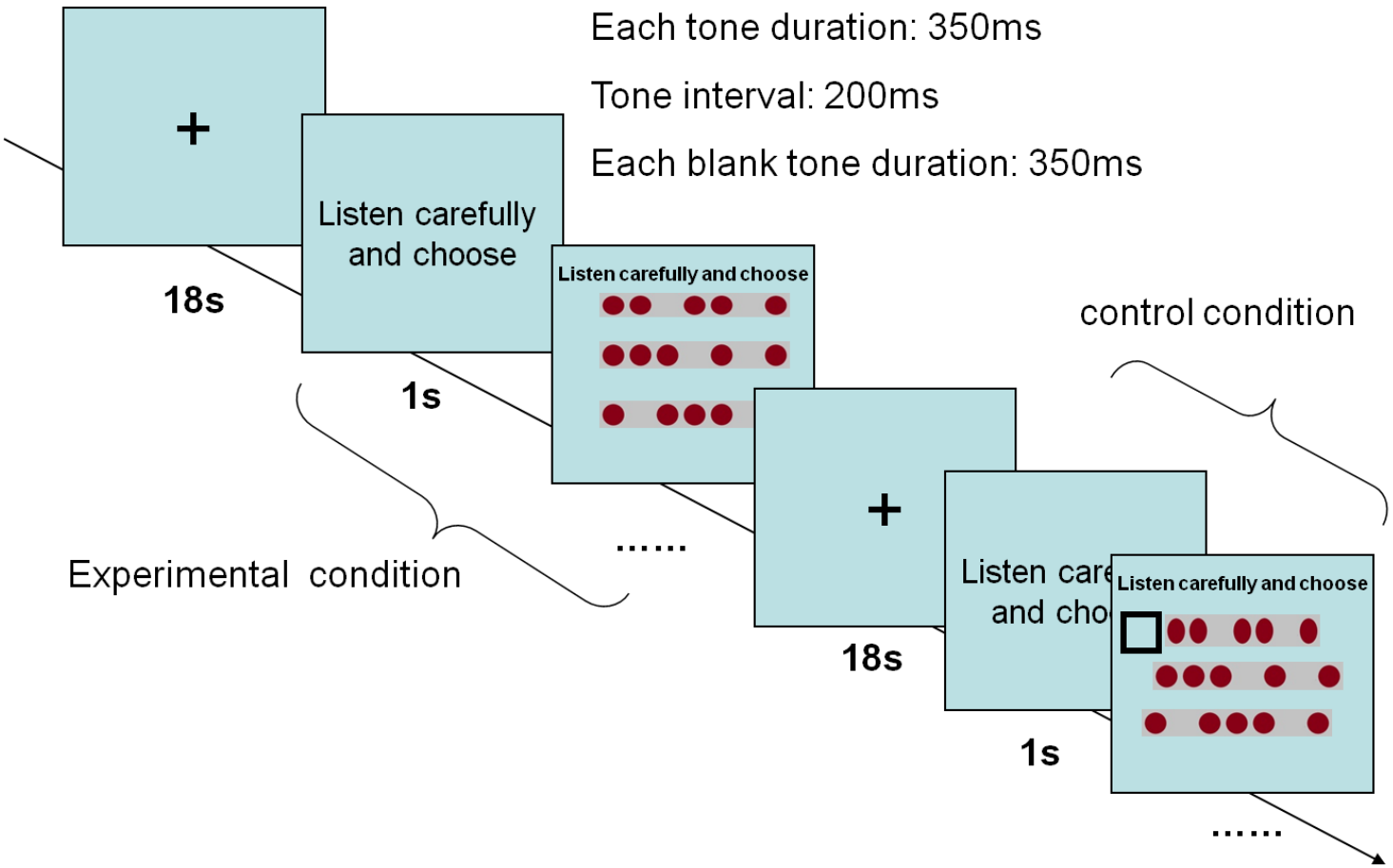

Figure 1: Illustration of the spatial-temporal information matching task which captures audiovisual sensory integration processing

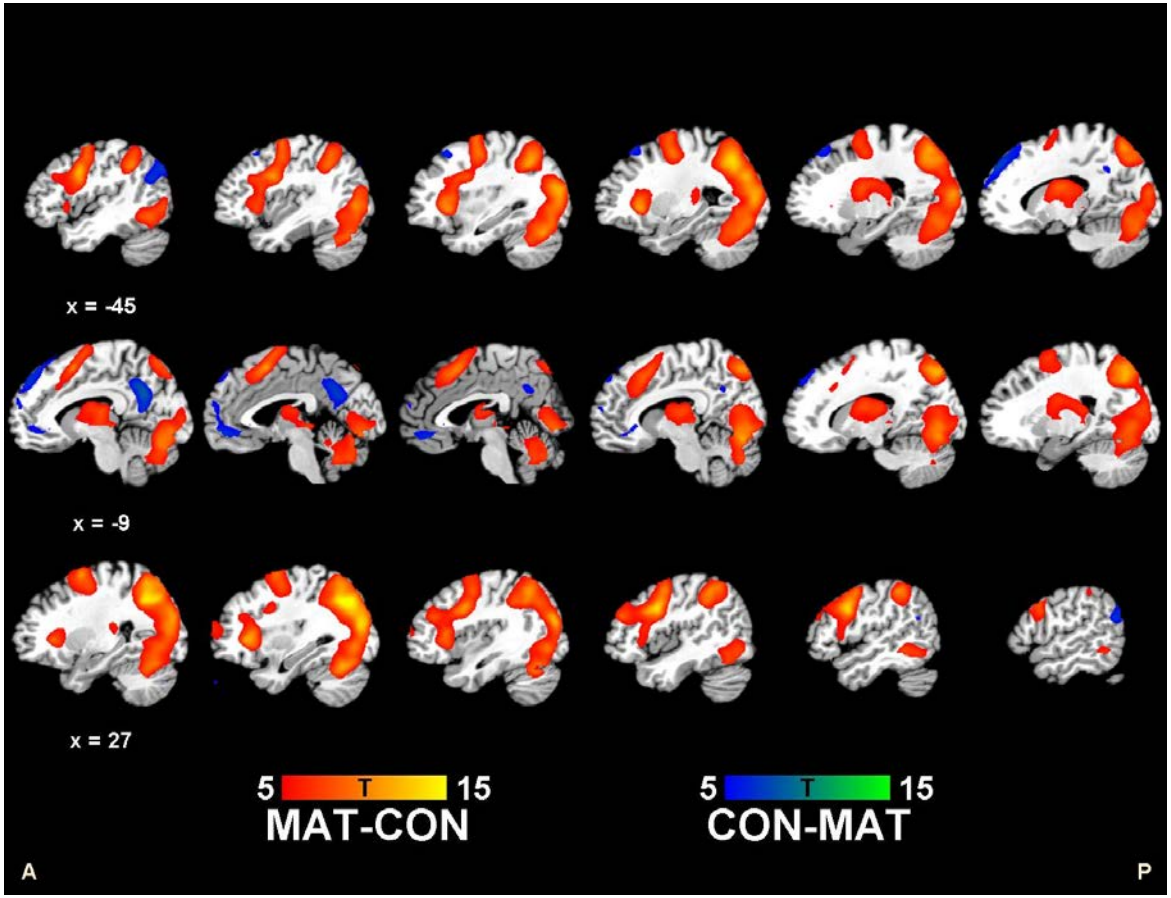

Figure 2: Sagittal view of whole brain activation pattern in contrasts between matching (MAT) and control (CON) conditions. Colour legend represents Z value in the activation clusters. All contrasts resulted from a random effect GLM in MNI coordinates

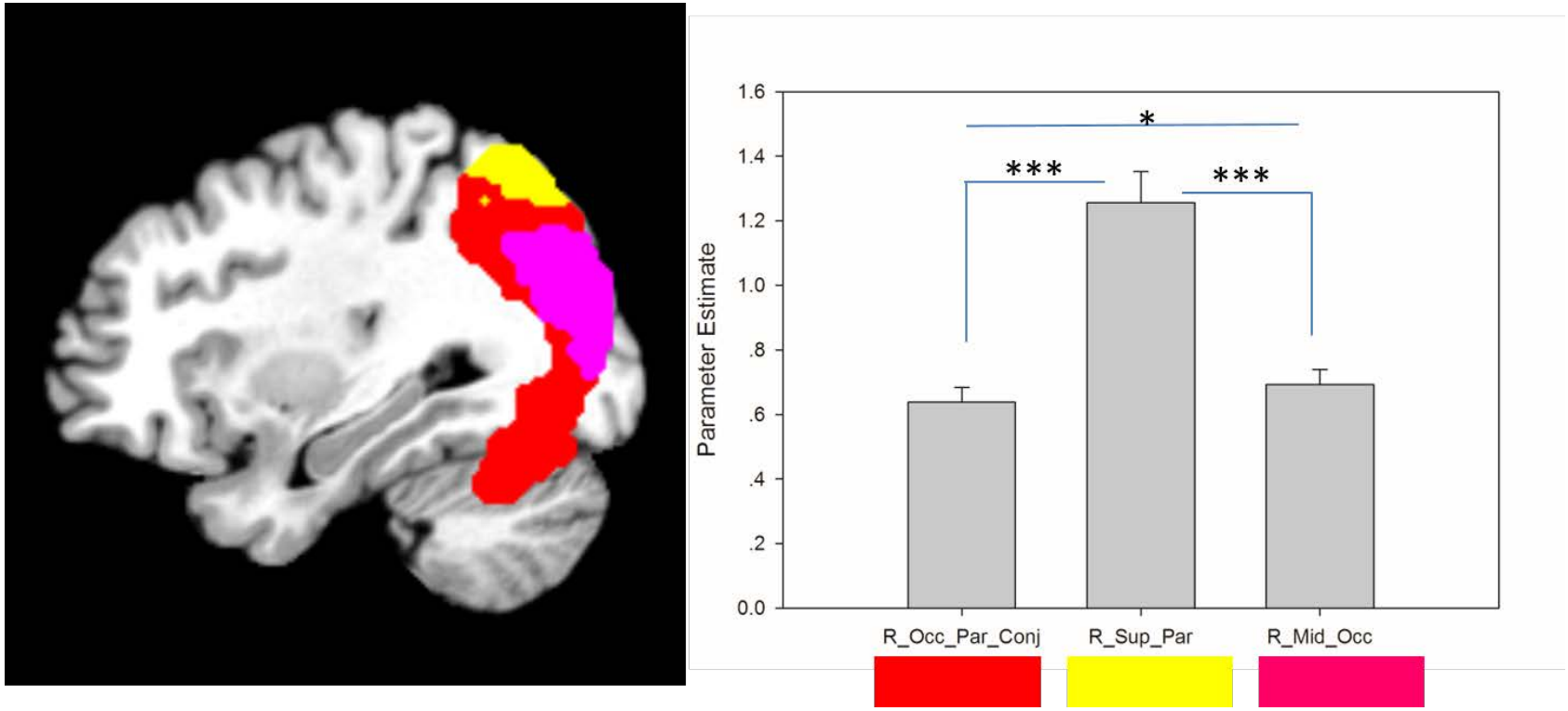

Figure 3: Three regions of interest and their parameters were estimated in the matching-control contrast. The red part represents the right occipital-parietal conjunction cluster. The yellow part represents the combination of the right occipital-parietal conjunction cluster and the right superior parietal lobe anatomically defined in AAL brain structure. The purple part represents the combination of the right occipital-parietal conjunction cluster and the right middle occipital lobe cluster anatomically defined by the AAL brain structure. The right panel represents the parameter estimates extracted from these three ROIs (Mean $\pm$ SE), showing that the activation of the red part involves both the parietal and occipital cortex, which is therefore labeled as the right occipital-parietal conjunction. (Note: *: $p<0.05$; **: $p<0.01$; ***: $p<0.001$)

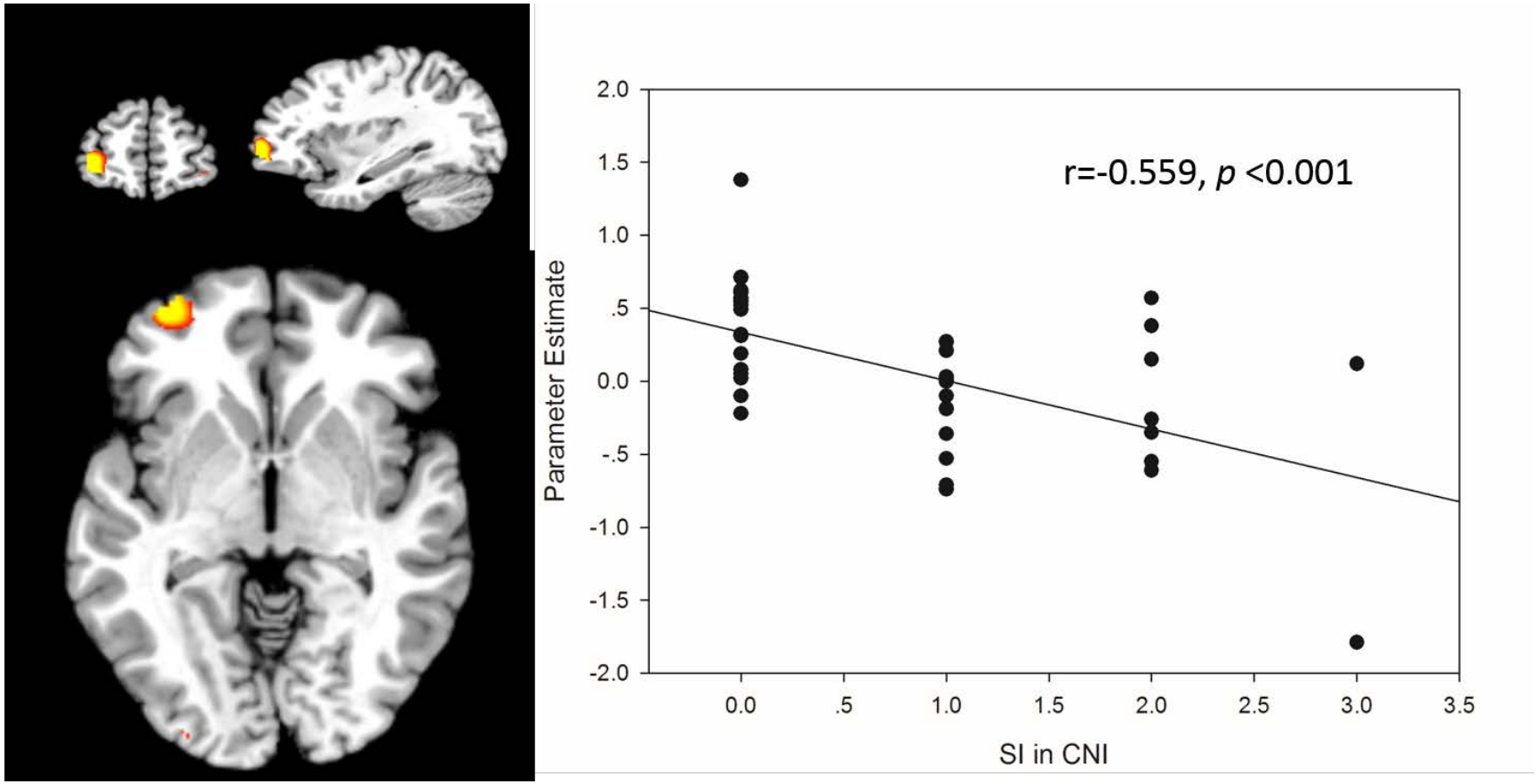

Figure 4: Results of the regression between the BOLD response (difference of the beta value between matching condition and control condition) and the score reported at the sensory integration subscale of the CNI (Left panel: left SFG, peak voxel: x, y, z=-40 56 -2, n=37, p<0.05, alphasim corrected on cluster level; Right panel: scatter plot, r=-0.559, p<0.001).